Shear-Induced Textures in the Lyotropic Liquid Crystal Poly(γ-benzyl L-glutamate) (PBLG)

N. X. Yan and M. M. Labes*

Department of Chemistry, Temple University, Philadelphia, Pennsylvania 19122

S. G. Baek and J. J. Magda

Department of Chemical and Fuels Engineering, University of Utah, Salt Lake City, Utah 84112

Received December 3, 1993; Revised Manuscript Received February 23, 1994®

ABSTRACT: Starting with large monodomain samples of PBLG with homeotropic alignment, the dynamics of textural evolution have been studied in detail at relatively low shear rates. A wide variety of textural patterns are seen which are explained by considering the appropriate balance of the elastic forces in the liquid crystal against the viscous forces due to shear flow. Textural evolution depends on shear rate and sample thickness.

Introduction

As a consequence of the many possibilities for application of liquid crystalline polymers (LCPs) in ultrahigh modulus fibers and nonlinear optics, many studies relating to the processing of the materials have been undertaken. Of particular interest has been the occurrence of a "banded texture" after the cessation of shear.[1-10] Alternative white and black stripes, perpendicular to the shear direction, can be seen when the sample is examined between crossed polars. It has been suggested that the banded structure is caused by the serpentine arrangement of molecules along the shear direction.[2] Since it is well-known that fibers extruded from LCP phases have superior mechanical properties, and also possess the banded structure,[2] there is clearly a need to understand the relationship between them. There have been a number of studies utilizing a variety of shearing processes[3-8] to attempt to elucidate the important parameters affecting the banded texture and hypothesize a reasonable mechanism for this phenomenon.[8-10]

A large number of investigations of the rheological properties of LCPs[11-28] have accompanied these shearing studies. In many of the experiments, theoretical predictions of Larson, Doi, and Marrucci regarding the rheological properties of LCPs have been confirmed. In contrast to typical small molecule liquid crystals, LCPs show tumbling behavior at low shear rates ($\dot{\gamma}$),[11-13] despite the molecules being quite large, and shear alignment at high shear rates. Since the molecules are large and the medium is of high viscosity, the defect domains can easily be driven by shear down to the molecular scale. In this way, nonlinear viscoelastic interactions between shear flow and the molecular orientation probability distribution function lead to peculiar stress behavior; namely under steady flow, one obtains a negative first normal stress difference[11,12,14-23] and a positive second normal stress difference.[14,15] This regime is located within the transition region from tumbling at low shear rates to shear alignment at higher shear rates. While in the linear region of low shear, tumbling motion leads to spatial twisting of the director, which in turn leads to a polydomain texture. This polydomain texture causes damped oscillatory responses to stress which scale with the shear strain in transient flow.[11,13,19,24]

Even though there are a number of investigations of the structure of LCPs under shear by light scattering[3,25] or birefringence measurements,[13,18,19,26] a precise picture is still not available. Recently Larson and Mead[27,28] studied LCP textures and their evolution under crossed polars, by shearing an initially coarsely textured sample at low shear rate. When the Ericksen number E was larger than a threshold value, the director flipped out of the shear plane in a manner which was dependent on its initial alignment. The variations of the texture under steady flow could be characterized by the values of E. These studies may explain unsolved puzzles such as the lower degree of molecular orientation with respect to the shear direction observed in steady flow,[18,29] and the initial increase of molecular orientation upon reversal of the flow direction.[19]

In this work, further investigation of LCP texture and its evolution under shear was undertaken by utilizing well-aligned monodomain samples and a widely varying shear rate. Textural evolution as a function of shear rate and sample thickness was directly characterized under crossed polars.

Experimental Section

Shearing Apparatus and Optical Microscopy. The shearing apparatus for a simple flow experiment is shown in Figure 1 and is similar in design to that described by Larson et al.[27] A precision step motor (SX-57 made by Parker Hannifin Corporation) is connected to a drive screw having 1 mm advance per turn, which in turn couples to the sample holder, driving the top plate. The motor is controlled by a computer and has a velocity within the range 0.0001–30 mm s^{-1} giving $\dot{\gamma}$ = 0.005–1500 s^{-1} when the sample thickness, h, is 20 μm.

The apparatus is placed on a rotatable microscope stage between two polars. Extinction of light occurs in those regions of the sample in which the director is parallel to one of the two crossed polars. For convenience in describing the experiment, one can adopt two reference frames. In the laboratory frame, the lower polarizer is along the direction x', and the upper polarizer is along y'. In the sample frame, the shearing direction is referred to as the x axis, and the vorticity direction, which is at an angle of 90° to the shear direction, is the y axis. The light path is thus along z' in the laboratory frame, and along z in the sample frame. If x is at an angle θ with x', extinction in a local region implies that the director in that region is also oriented at an angle $-\theta$ or $-\theta + 90°$ with respect to the shear direction. This ambiguity can be removed by following the shift in the field color when a quarter wave plate with λ = 5300 Å is inserted and the sample is rotated. If a quarter wave plate with its slow axis at 45° with respect to the polar (x') is inserted, the originally dark field becomes pink.

® Abstract published in *Advance ACS Abstracts*, April 1, 1994.

0024-9297/94/2227-2784$04.50/0

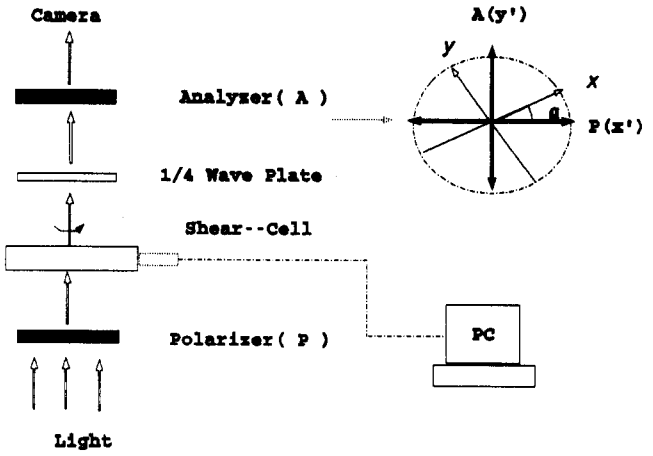

Figure 1. Experimental apparatus.

After the sample is rotated toward the slow axis of the quarter wave plate, the pink field becomes orange or blue when the director originally is at $-\theta$ or $-\theta + 90°$ with respect to the x axis. By rotating the sample and observing the change in the extinction regions of the sample, one can determine the director distribution both during and after shear.

Sample Preparation. PBLG was obtained from Sigma Chemical Company and used without further purification. It was dissolved in a 42/58 (v/v) mixture of dioxane and nitrobenzene at a concentration of 20% (g/mL) to afford a nematic phase of this optically active polymer by virtue of solvent compensation.[30] Samples were made from PBLG of two different molecular weights (MWs): PBLG(248K) represents a MW of 248 000 and PBLG(187K) represents a MW of 187 000. The samples were sealed in ampoules and incubated at room temperature for more than 2 weeks.

A sandwich consisting of two microscope slides with an electrically conductive coating of a mixture of tin and indium oxides were used as substrates. The only significance of the coating in these experiments is to provide excellent homeotropic alignment of PBLG (even without application of an electric field). The origin of this effect[31] may lie in the strong electrostatic interaction of the charged groups in PBLG with the ionic charges on the surface of metal dioxide films as compared to those on the surface of an uncoated SiO_2 plate. The sample was placed into such a cell with the slides separated by Teflon spacers created by masking the central area of the slides and spray coating the remainder with a Teflon spray (Crown Industrial Inc.). The accuracy of the spacer could be controlled to within 2 μm. Such samples can be kept for a week without any appreciable loss of solvent. After the sample was presheared several times at $\dot{\gamma}$ of about 100 s^{-1} and then allowed to relax for 3–4 h, a homeotropic alignment is observed in the sample. The area of a PBLG monodomain achieved in this manner can easily be greater than 1 cm^2.

Rheology. The rheological measurements on the nematic PBLG(187K) were performed utilizing a cone-and-plate rheometer on polydomain samples. The thickness of the sample in such an instrument increases linearly with radial position, from 50 μm at the cone tip to 0.87 mm at the cone rim. The viscosity and the first normal stress difference of PBLG(187K) vs shear rate are shown in Figure 2. The shear thinning region and the maximum negative value of the first normal stress difference for PBLG(187K) occur at $\dot{\gamma}$ larger than 1000 s^{-1}. Based on these data and on previous work,[19,20,28] it is reasonable to conclude that PBLG(248K) would have a $\dot{\gamma}$ of about 80 s^{-1}. Unfortunately because of experimental limitations, the rheological measurements could not be performed over the entire region of shear rates used in the rheooptical experiments. Figure 2 indicates that the value of $\dot{\gamma}$ used in the rheooptical experiment is within the tumbling region, since it is below 50 s^{-1}. With such a shear rate, textural evolution for both molecular weights 187K and 248K are rather similar with a sample thickness of 20 μm, except that $\dot{\gamma}_{c1}$ and $\dot{\gamma}_{c2}$ for PBLG(187K) shift to slightly higher values. $\dot{\gamma}_{c1}$ and $\dot{\gamma}_{c2}$ are the threshold shear rates dividing the shear regime into three regions which differ in the character of the textural evolution. For simplicity, we consider below only the results for PBLG(248K).

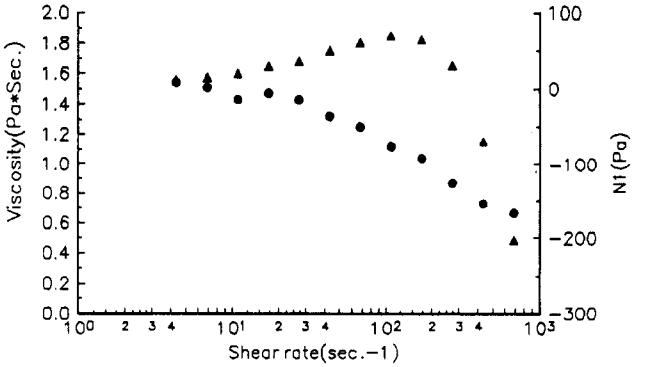

Figure 2. Viscosity and N1, the first normal stress difference, as a function of shear rate for PBLG(187K) at a concentration of 20% (wt/vol) in 42/58 (vol/vol) dioxane/nitrobenzene. A cone–plate rheometer (Modified R-17 Weissenberg rheogoniometer) was employed. ▲ = viscosity, ● = N1.

Textural Evolution during Shear. There is a diversity of behavior in the evolution of textural features which depends on shear rate. For convenience in discussion, the variation of textural evolution vs shear rate can be divided into three distinct regimes: Region **A** with $\dot{\gamma} \leq \dot{\gamma}_{c1}$, region **B** with $\dot{\gamma}_{c1} < \dot{\gamma} \leq \dot{\gamma}_{c2}$, and region **C** with $\dot{\gamma} > \dot{\gamma}_{c2}$. The results obtained with PBLG(248K) with a sample thickness of $h = 20$ μm and an initial homeotropic alignment are given below.

Region A with $\dot{\gamma} < \dot{\gamma}_{c1} = 0.05$ s^{-1}. With shear flow occurring in the direction x', immediately upon initiating shear, the original uniform dark field under crossed polars remains the same in the x–y plane. When the sample is rotated with respect to the polars, the uniform dark field becomes bright. Therefore, the director appears to be rotated within the shear plane (the x–z plane), and the alignment is uniform in the x–y plane.

Region B with 0.05 $s^{-1} \leq \dot{\gamma} < \dot{\gamma}_{c2} = 0.5$ s^{-1}. In this region, the director flips out of the shear (x–z) plane in a nonuniform way in the x–y plane and is further rotated by the local viscoelastic fields. A complex nonlinear evolution of the texture occurs before the formation of disclinations. The textures which are observed under crossed polars with the optic axis of the lower polar parallel to the shear direction at $\dot{\gamma} = 0.2$ s^{-1} are shown as a function of shearing time in Figure 3.

At first, the director rotates in the shear plane (x–z plane); after approximately 100 s, the director flips out of the shear plane resulting in the bands shown in Figure 3a. In this banded structure, the director arranges in a zigzag fashion along the direction of shear flow (the x direction). The band spacing is about 40 μm, which is approximately two times the sample thickness. The maximum angle made by the director with the direction of shear flow is less than 10°. Fine bands parallel to the shear flow direction follow immediately; the texture observed at 170 s is given in Figure 3b. The alignment of the director varies periodically in the y direction orthogonal to the shear flow direction with an angle of 20° and a band spacing of about 10 μm. These bands then disappear and are replaced by a uniform dark field. Originally, the dark field under crossed polars becomes bright when the sample is rotated, indicating that the director is parallel to either one of the crossed polars. The behavior of the sample upon insertion of a quarter wave plate, described in detail in the Experimental Section, indicates that the director is, once again, confined within the x–z plane.

After further shear for 280 s, the texture shown in Figure 3c develops, which is rather similar to that shown in Figure 3a, except that the band spacing is now about 20 μm, and the maximum angle of the director with the shear direction is now about 30°. In certain areas of the sample (the **A** area in Figure 3d), this angle continuously increases until disclinations perpendicular to the shear direction are formed at 350 s. Under further shear, these disclinations tend to align along the shear direction. In other areas of the sample (the **B** area in Figure 3d), a uniform texture forms and bands parallel to the shear direction appear again. After further shear, disclinations are formed in the latter area, or the area shrinks until disclinations uniformly fill up the space. After prolonged shear, these disclinations align along the shear direction and give the "striped" texture shown

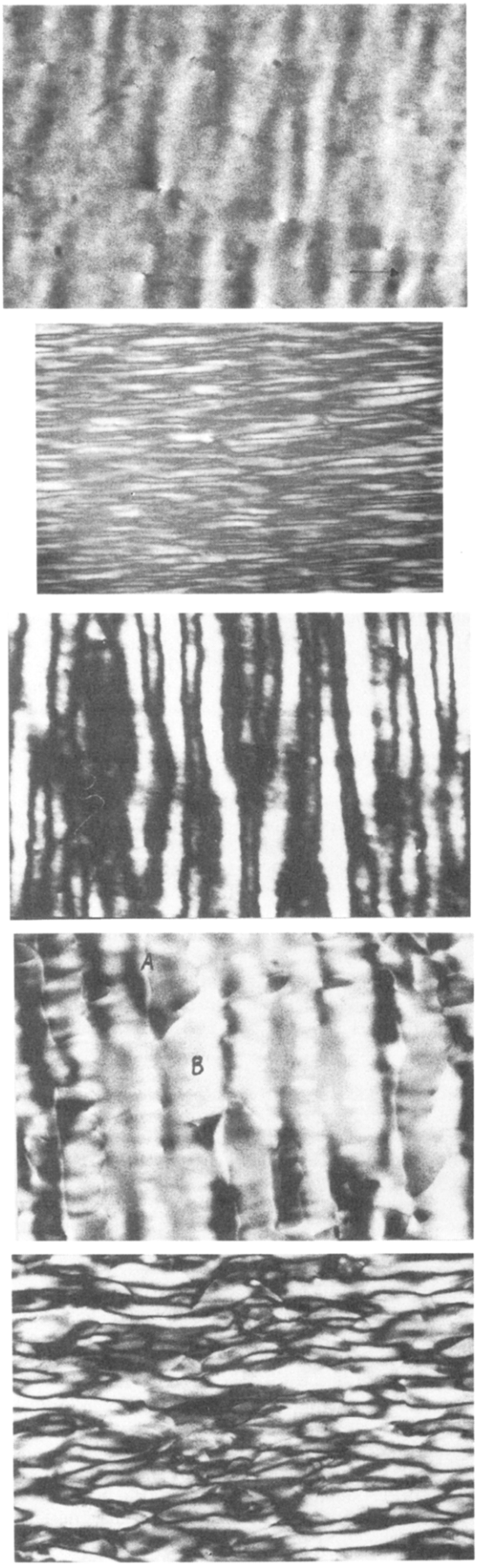

Figure 3. Photomicrographs of PBLG(248K) sheared at 0.2 s^{-1} taken with crossed polars with the lower polar parallel to the shear flow direction: (a, top) 100 s after the initiation of shear flow; (b, near top) 170 s; (c, middle) 280 s; (d, near bottom) 350 s; and (e, bottom) 800 s. The bar drawn in (a) is 50 μm long, and the arrow represents the shear direction.

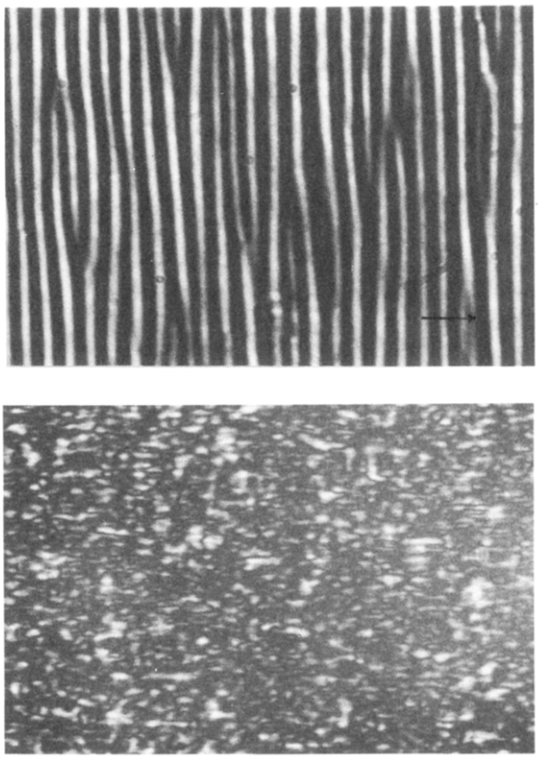

Figure 4. Photomicrographs of PBLG(248K) sheared at 1.0 s^{-1} taken under crossed polars with the lower polar parallel to the shear flow direction: (a, top) 30 s after the initiation of shear flow and (b, bottom) 130 s. The bar drawn in (a) is 50 μm long, and the arrow represents the shear direction.

Table 1. Dependence of the Shear Rates $\dot{\gamma}_{c1}$ and $\dot{\gamma}_{c2}$ on Sample Thickness for PBLG(248K)

thickness (μm ± 2)	$\dot{\gamma}_{c1}$ (s^{-1})	$\dot{\gamma}_{c2}$ (s^{-1})
10	0.24	2.2
20	0.05	0.50
30	0.03	0.3
40	0.02	0.1

in Figure 3e. This striped texture has also been well characterized earlier.[27,28]

Region C 0.5 $s^{-1} \leq \dot{\gamma} < 50$ s^{-1}. At the beginning of the shearing process in this region, one observes essentially the same behavior as is encountered in region B until bands perpendicular to the shear direction have formed. After 30 s, the texture observed with $\dot{\gamma} = 1.0$ s^{-1} is shown in Figure 4a. But the maximum angle of the bands with respect to the flow direction increases so that defects are formed. A texture similar to that of Figure 3d appears first and is then followed by one similar to that of Figure 3e. With further shear at these high shear rates at 130 s, a polydomain texture (Figure 4b) appears. Without an analyzer, or by rotating the sample, the sample has a bright field with very short thin black or white lines. Obviously the texture in Figure 4b is caused by director turbulence, as has been also observed by Larson and Mead.[28]

Discussion

Textural Evolution during Transient Flow. As described in the last section, LCP textures and their evolution vary with shear rate. There is also a thickness dependence of the values of $\dot{\gamma}_{c1}$ and $\dot{\gamma}_{c2}$ which are given in Table 1. Both of these quantities are inversely proportional to the square of the sample thickness. It is obvious that they correlate with the spatial variation of the director and the viscoelastic field along z.

The shear rates used in these experiments are smaller than the threshold value at which N1 reaches its maximum negative value, implying that textural evolution is determined by a combination of a Frank elastic torque due to spatial variation of the director and a viscous hydrody-

namic torque associated with shear flow. In this region, textures can be associated with an Ericksen number $E = \gamma_1 \dot{\gamma} h^2/K_1$.[28] Here, γ_1 is the rotational viscosity, h is the sample thickness, and K_1 is the Frank splay constant. Previous measurements give a value for $\gamma_1/K_1 \sim 1\ \mu m^2\ s^{-1}$ for PBLG(248K).[32] The value of E corresponding to $\dot{\gamma}_{c1}$ is about 25 at which the director starts to rotate out of the shear plane and roll cells are formed. E corresponding to $\dot{\gamma}_{c2}$ is about 200 $\mu m^2\ s^{-1}$ and is found at the onset of director turbulence. After shear starts, the director, which has an initial homeotropic alignment, rotates under the torque produced by the viscous field. Because of strong boundary anchoring, the director is pinned near the wall and varies along the z direction so as to be in accord with the Frank elasticity. In turn this elasticity tends to balance against the viscous shear torque. When $\dot{\gamma} < \dot{\gamma}_{c1}$ (region **A**), there is a stable alignment even after prolonged shear. The director is confined in the shear plane (x–z plane) and is uniform in the sample plane (the x–y plane). This stability was theoretically shown by Marrucci.[22] When $\dot{\gamma} > \dot{\gamma}_{c1}$ (regions **B** and **C**), there is an elastic instability for the director deviation out of the shear plane which is similar to that proposed by Zúñiga and Leslie.[29] When $\dot{\gamma} > \dot{\gamma}_{c2}$, the shear distortion is so severe that disclinations immediately follow after the formation of perpendicular bands. When $\dot{\gamma}_{c1} < \dot{\gamma} < \dot{\gamma}_{c2}$, the director rotates under the local elastic field and shear flow. As a consequence of the complex nonlinear evolution of texture, bands perpendicular and parallel to the shear flow direction appear alternately, as shown in Figure 3, before the formation of defects.

When $\dot{\gamma} > \dot{\gamma}_{c2}$, the appearance of the bands in Figure 4a scales with the total shear strain (shear rate × shear time), as has been previously noted.[27] The total shear strain starting with an initial homeotropic alignment is about 30 for PBLG(248K) and 25 for PBLG(187K) but barely varies with sample thickness, in contrast with previous measurements.[27] Since the evolution of the textures during initial flow scales with the total shear strain, it appears that associated physical quantities like viscosity and N1 may vary with the same scaling rule. Rheological measurements that have been performed under transient flow[11,13,19,24] do not start with a monodomain, so that the damped oscillation of the viscous torque and the first normal stress difference are values averaged within these initial polydomains. With different initial alignment before shear, it has been shown that the textural evolution still scales with the total shear strain.[27] This implies that variations in the mechanical parameters averaged over these polydomains also follow a scaling rule with shear strain. This phenomenological discussion leads to the idea that the textural evolution shown in these experiments is intrinsically related to the damped oscillation of the viscosity upon the initiation of shear flow.

Texture under Steady Flow. A stable texture, uniform in the x–y plane as a result of the equilibration of Frank elasticity with the flow-induced torque, is seen in the experiments when $\dot{\gamma} < \dot{\gamma}_{c1}$. In this case, the viscosity basically is invariant with shear rate[22,26] differing from the behavior in viscosity region I where shear-thinning effects occur at low shear rates when the director is not constant along the shear direction. Since $\dot{\gamma}_{c1}$ is dependent on sample thickness, the occurrence of viscosity region I depends on the geometry of the rheometer.

When $\dot{\gamma} > \dot{\gamma}_{c1}$, as shown in Figures 3e and 4b, disclinations are formed and align along the shear direction after prolonged shear. These defect lines shorten with increasing shear rate and have a high number density. Under crossed polars, with the lower polar in the direction of shear, the "striped" texture seen in Figure 3e continuously transforms into a turbulent texture shown in Figure 4b, similar to that observed recently by Larson and Mead.[28] When the shear rate is higher than $\dot{\gamma}_c$, this polydomain texture has a preferred orientation in which the director is confined to a small angle with respect to the shear flow direction. When the sample is rotated under crossed polars, the features shown in Figures 3e and 4b become closed dark circles against a bright background. Upon further rotation, the circles shrink and become smaller. When the sample is rotated by the angle θ_c with respect to the lower polar, the texture seen in Figure 4b changes to show tiny dark spots against a bright background. In contrast, Figure 3e does not change in this way. θ_c obviously represents the maximum angle of director deviation from the shear direction in the polydomain texture of Figure 4b. It should be pointed out that $\dot{\gamma}_c$ is not the same as either $\dot{\gamma}_{c1}$ or $\dot{\gamma}_{c2}$ and is not sensitive to the sample thickness. $\dot{\gamma}_c$ has a value of about 1 s^{-1} for PBLG(248K). An analysis of the change in θ_c vs shear rate is presented in Figure 5. Several conclusions can be drawn. (1) θ_c decreases with increasing shear rate until it reaches a constant value of 15° when $\dot{\gamma} \geq 10\ s^{-1}$. (2) The behavior is not sensitive to sample thickness. (3) In comparison to Figure 2, the region of strong variation of θ_c with shear rate corresponds to the plateau region of the viscosity curve. Although the macroscopic quantities such as molecular orientation[18] and viscosity do not change with shear rate, the textures of the LCPs show a marked dependence. After cessation of shear, bands perpendicular to the shear flow appear. Therefore $\dot{\gamma}_c$ corresponds to the threshold shear rate for the formation of perpendicular bands after the cessation of shear.[1-10] These banded domains form faster and become larger with increasing shear rate.

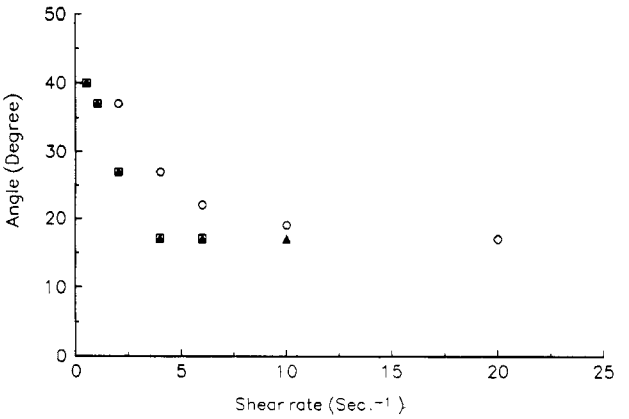

Figure 5. θ_c vs shear rate for PBLG(248K). ▲ = θ_c at a sample thickness of 10 μm; □, 20 μm; ○, 30 μm.

Conclusions

Textural evolution in LCPs caused by shearing a single domain with homeotropic alignments have been studied in detail at low shear rates. After the initiation of flow, textural evolution depends on both shear rate and sample thickness. $\dot{\gamma}_{c1}$ and $\dot{\gamma}_{c2}$ are inversely proportional to the square of the sample thickness and yield corresponding Ericksen numbers of 25 and 200. Larson and Mead report values of 25–50 for the formation of roll cells and >500 for director turbulence on PBLG–PBDG samples which involve different solvents and slightly different molecular weights.[28] The observed patterns can be explained by considering a balance of the elastic torque due to spatial distortion of the director field against the viscous torque due to shear flow.

In the steady flow regime, a stable configuration which is uniform in the x–y plane is reached in region **A** where

$\dot{\gamma} < \dot{\gamma}_{c1}$. When $\dot{\gamma} > \dot{\gamma}_{c1}$, disclination lines are formed parallel to the shear direction. At higher shear rates, disclinations along the shear direction become shorter, and the "striped" texture observed under crossed polars continuously transforms into a "turbulent" texture. When $\dot{\gamma} > \dot{\gamma}_c$, the director fields of the polydomains become confined within small angles about the shear flow direction. $\dot{\gamma}_c$ corresponds to the threshold shear rate for the formation of the banded structure after the cessation of shear. All of these phenomena are observed when the viscosity vs shear rate curve reaches a plateau region.

Acknowledgment. The work at Temple University was supported by the National Science Foundation under Grant No. DMR-93-12634. The assistance of E. Kaczanowicz in apparatus design and construction and valuable discussions with M. Kuzma are gratefully acknowledged.

References and Notes

(1) Elliott, A.; Ambrose, E. J. *Disc. Faraday Soc.* **1950**, *9*, 246.
(2) Horio, M.; Ishikawa, S.; Oda, K. J. *Appl. Polym. Symp.* **1985**, *41*, 269.
(3) Ernst, B.; Navard, P. *Macromolecules* **1989**, *22*, 1419.
(4) Marrucci, G.; Grizzuti, N.; Buonurio, A. *Mol. Cryst. Liq. Cryst.* **1987**, *153*, 263.
(5) Marsono, E.; Carpaneto, L.; Cifferi, A. *Mol. Cryst. Liq. Cryst.* **1988**, *158B*, 267.
(6) Fincher, C. R., Jr. *Mol. Cryst. Liq. Cryst.* **1988**, *155*, 559.
(7) Donald, A. M.; Viney, C.; Ritter, A. P. *Liq. Cryst.* **1986**, *1*, 287.
(8) Gleeson, J. T.; Larson, R. G.; Mead, D. W.; Kiss, G.; Cladis, P. E. *Liq. Cryst.* **1992**, *11*(3), 341.
(9) Zielinska, B. J. A.; Bosch, A. T. *Liq. Cryst.* **1989**, *6*(5), 533.
(10) Picken, S. J.; Moldenares, P.; Berghmans, S.; Mewis, J. *Macromolecules* **1992**, *25*, 4759.
(11) Marrucci, G. *Liquid Crystallinity in Polymers*; VCH Publishers, Inc.: New York, 1991; p 395.
(12) Srinivasarao, M.; Berry, G. C. *J. Rheol.* **1990**, *35*, 379.
(13) Burghardt, W. R.; Fuller, G. G. *Macromolecules* **1991**, *24*, 2546.
(14) Larson, R. G. *Macromolecules* **1990**, *23*, 3983.
(15) Magda, J. J.; Baek, S. G.; De Vries, K. L.; Larson, R. G. *Macromolecules* **1991**, *24*, 4460.
(16) Marrucci, G.; Maffettone, P. L. *J. Rheol.* **1990**, *34*, 1217.
(17) Kiss, G.; Porter, R. S. *J. Polym., Sci. Polym. Symp.* **1978**, *65*, 193.
(18) Hongladarom, K.; Burghardt, W. R.; Baek, S. G.; Cementwala, S.; Magda, J. J. *Macromolecules* **1993**, *26*, 772.
(19) Hongladarom, K.; Burghardt, W. R. *Macromolecules* **1993**, *26*, 785.
(20) Doi, M.; Edwards, S. F. *J. Chem. Soc., Faraday Trans.* **1978**, *74*, 560; **1978**, *74*, 918.
(21) Doi, M.; Edwards, S. F. *The Theory of Polymer Dynamics*; Clarendon Press: Oxford, 1986; p 350.
(22) Marrucci, G. *Macromolecules* **1991**, *24*, 4176.
(23) Larson, R. G.; Doi, M. J. *J. Rheol.* **1991**, *35*, 539.
(24) Doppert, H. L.; Picken, S. J. *Mol. Cryst. Liq. Cryst.* **1987**, *153*, 109.
(25) Takebe, T.; Hashimoto, T.; Ernst, B.; Navard, P.; Stein, R. S. *J. Chem. Phys.* **1992**, *92*(2), 1386.
(26) Onogi, S.; Asada, T. *Rheology*; Plenum Press: New York, 1980; Vol. 1, p 127.
(27) Larson, R. G.; Mead, D. W. *Liq. Cryst.* **1992**, *12*(5), 751.
(28) Larson, R. G.; Mead, D. W. *Liq. Cryst.* **1993**, *15*(2), 151.
(29) Zúñiga, I.; Leslie, F. M. *Liq. Cryst.* **1989**, *5*(2), 725.
(30) Robinson, C. *Trans. Faraday Soc.* **1956**, *25*, 571.
(31) Dupré, D. B. In *Polymer Liquid Crystals*; Cifferi, A., Krigbaum, W. R., Meyer, R. B., Eds.; Academic Press, Inc.: New York, 1982; p 186.